PROCEEDINGS OF THE ROYAL SOCIETY A

Proc. R. Soc. A (2006) **462**, 3233–3251
doi:10.1098/rspa.2006.1708
Published online 5 May 2006

Crack-front instability in a confined elastic film

By M. Adda-Bedia[1] and L. Mahadevan[2,*]

[1]*Laboratoire de Physique Statistique de l'Ecole Normale Supérieure, 24 rue Lhomond, 75231 Paris, France*
[2]*Division of Engineering and Applied Sciences, Harvard University, Pierce Hall, 29 Oxford Street, Cambridge, MA 02138, USA*

We study the undulatory instability of a straight crack front generated by peeling a flexible elastic plate from a thin elastomeric adhesive film. We show that there is a threshold for the onset of the instability that is dependent on the ratio of two length-scales that arise naturally in the problem: the thickness of the film and an elastic length defined by the stiffness of the plate and that of the film. A linear stability analysis predicts that the wavelength of the instability scales linearly with the film thickness. Our results are qualitatively and quantitatively consistent with recent experiments, and show how crack fronts may lose stability due to a competition between bulk and surface effects in the presence of multiple length scales.

Keywords: fracture; peeling; adhesion; instability

1. Introduction

The problem of peeling a thin plate from a soft confined adhesive film arises repeatedly in a number of scientific and technological applications, ranging from the ubiquitous band-aid to insect foot-pads. In these systems, peeling separates the joined solids and failure occurs via the loss of adhesion at one of the surfaces attached to the adhesive. When the intercalating adhesive material between the plate and the substrate is a fluid or viscoelastic solid, early studies on peeling (McEwan & Taylor 1966; Fields & Ashby 1976; Conley *et al.* 1992) drew an analogy to the Saffman–Taylor problem (Saffman & Taylor 1958) for the dynamics of an interface between two fluids in a confined geometry. Recent experiments with purely elastic intercalating materials (Ghatak *et al.* 2000; Monch & Herminghaus 2001; Ghatak & Chaudhury 2003) have shown that static patterns almost identical to those observed in the Saffman–Taylor problem arise at the peeling interface. In figure 1*a*, we show the schematic for such an experiment where a thin flexible cover-slip is peeled off from a soft, thin elastic adhesive film that is itself attached firmly to a rigid substrate. Examples of the resulting complex crack morphologies that arise are shown in figure 1*b*. An important qualitative difference is that the difference between the fingering in

* Author for correspondence (lm@deas.harvard.edu).

Received 7 June 2005
Accepted 3 March 2006

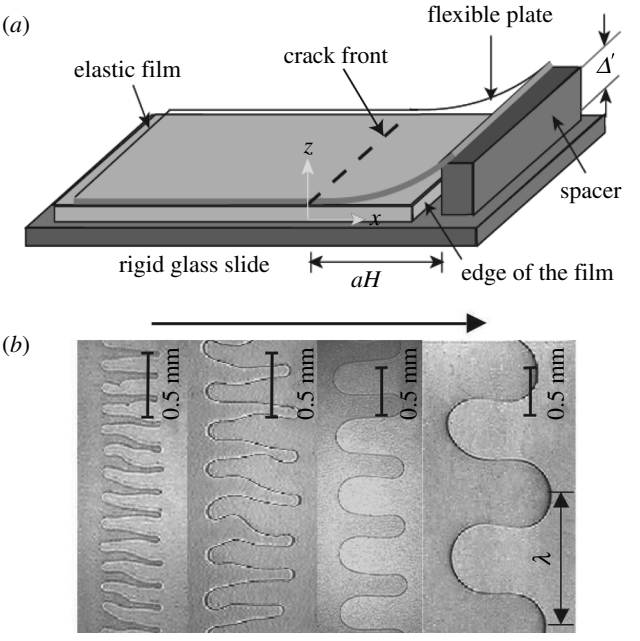

Figure 1. (*a*) Schematic of the problem. (*b*) The crack front loses stability to an undulatory mode when the confinement parameter $\alpha = (D/\mu H^3)^{1/3}$ is large enough. The various morphologies correspond to increasing thicknesses of the adhesive film for a given flexural stiffness of the cover-slip. Typical experimental parameter values are $20 \ll \alpha \ll 100$, and a film thickness $H \sim 50\ \mu$m. See Ghatak & Chaudhury (2003) for further details. (Figure courtesy of A. Ghatak & M. Chaudhury.)

elastomeric films shown in figure 1*b* and that in fluid or viscoelastic films is that the former does not involve the transport of matter and is a purely elastic instability that is rate independent, unlike the Saffman–Taylor instability and its cousins which are strongly rate dependent. Recent attempts to understand these purely elastic interfacial patterns have focused on the case of two rigid solids separated by a thin adhesive layer (Ghatak *et al.* 2000; Shenoy & Sharma 2002), and account for the detailed short-range interfacial forces using a combination of analytical (energetic) and computational analyses. However, the simplest occurrence of this instability in the context of an undulatory crack at peeling front, documented by Ghatak *et al.* (2000) and Ghatak & Chaudhury (2003), has not been analysed theoretically (but see Ghatak (2005)). In this paper, we present a continuum elastic analysis of the stability of a linear crack front in a confined elastic film. Our main result is a simple criterion for the instability of the peeling front or crack to planar undulations and follows from the effects of elastic confinement due to the presence of lateral boundaries. This result is independent of the detailed microscopic interfacial interactions, and is thus very general and applicable to a variety of different systems.

For relatively thick films in contact with soft elastic plates, the peeling front or crack is a straight line. However, for confined films in contact with stiff plates, the front loses the stability to an undulating geometry as can be seen in figure 1*b*. To understand this, consider a plate with bending stiffness D in contact with an elastomeric film of shear modulus μ and infinite thickness. When the plate is deformed by an amount δ over a characteristic length-scale l_{p}, the deformations

decay exponentially into the bulk of the elastomer with a scale l_p. To determine this, we equate the bending energy per unit width in the plate $D\delta^2/l_p^3$ with that in the elastomer $\mu(\delta/l_p)^2 l_p^2$ so that $l_p \sim (D/\mu)^{1/3}$ defines the penetration depth of the surface deformations. For an adhesive layer of finite thickness H, this allows us to define a 'confinement' parameter $\alpha = (D/\mu H^3)^{1/3}$; the larger this parameter, the more confined the system is. Experiments (Ghatak *et al.* 2000; Ghatak & Chaudhury 2003) show that the instability arises only if $\alpha > \alpha_c$, independent of the nature of the loading. The wavelength of the instability is found to be independent of all parameters and scales linearly with the film thickness H. To understand the qualitative nature of this phenomenon we note that when $\alpha \ll 1$, the film is unconfined and can accommodate a straight peeling front; indeed the related analysis of a crack front in an infinite three-dimensional solid shows that a straight crack is stable to small perturbations of its shape (Rice 1985). However, the introduction of a length-scale via confinement changes matters qualitatively. When $\alpha \gg 1$, the penetration depth is no longer l_p, but is instead H; this geometrical confinement induces large stresses in the neighbourhood of the crack front which decay exponentially away from this region. This allows the crack to explore other configurations to relieve the stored elastic energy and possibly become unstable. The role of confinement is to favour shear deformations over normal deformations; to accommodate the local squeezing of the elastic film at the crack-front, the crack prefers to undulate, since the excess cost of the undulation is more than made up by the energy released in the adhesive film, an effect that we will quantify in some detail.

In §2, we formulate the problem for the equilibrium of the flexible plate in partial contact with the elastomeric adhesive film. We assume that the film is an incompressible linearly elastic solid, and that the plate is bent weakly so that the curvature of the plate is small (and primarily in one direction). Then, we set-up the problem for the linear stability analysis of an initially straight crack front to small in-plane sinusoidal perturbations and determine the stress field in the film in terms of the plate-induced boundary displacement field. In §3, we determine the solution corresponding to the straight crack front, and in §4 we determine the perturbed local stress field due to a wavy perturbation of the crack front. When expressed in terms of stress intensity factors, our solution leads to a criterion for the stability of the crack front and yields both a critical confinement threshold and the wavelength of the perturbation. In §5, we summarize our results and put them in the larger perspective of crack-front stability in confined systems.

2. Formulation of boundary-value problem

The geometry of peeling pertinent to our problem shown in figure 1*a* shows the two length-scales in this problem: the thickness of the adhesive film H and a characteristic dimension determined by the balance between the energy of bending the cover-slip and the energy of stretching/shearing the adhesive film, given by $l_p = (D/\mu)^{1/3}$, where μ is the elastomer shear modulus and D is the flexural rigidity of the plate. The first length-scale characterizes variations in the vertical or z-direction while the second characterizes variations in the plane of the crack, i.e. along the (x, y)-directions. The experiments of Ghatak & Chaudhury (2003) show that the ratio of these length-scales determines the

onset of the instability which occurs when $l_p \geq 18H$. Although the vast disparity of these two length-scales at the onset of the instability ($H \ll l_p$) suggests that an elastic lubrication approximation similar to that used in Ghatak *et al.* (2004) should be sufficient for analysing the present problem, we shall see that some aspects of the problem are closely related to the behaviour of the stress field in the vicinity of the crack front, where the lubrication approximation clearly breaks down. Thus, we will not use the lubrication approximation here.

To make the problem dimensionless, we scale the coordinates $x_i \equiv (x, y, z)$ using H, and scale the displacements in the adhesive film $u_i \equiv (u, v, w)$ and the deflection of the flexible cover-slip $h(x, y)$ using Δ', the separation between the film and the plate at the spacer. We assume that the adhesive layer may be modelled as a linear incompressible elastic solid, and scale the stresses in it by $\mu\Delta'/H$. Then, we may write the scaled constitutive equation for the adhesive elastic layer as

$$\sigma_{ij} = -P\delta_{ij} + \frac{\partial u_i}{\partial x_j} + \frac{\partial u_j}{\partial x_i}, \tag{2.1}$$

and the equilibrium equations in the film and the condition of incompressibility are

$$\nabla P = \Delta \boldsymbol{u}, \tag{2.2}$$

$$\nabla \cdot \boldsymbol{u} = 0. \tag{2.3}$$

Combining equations (2.2) and (2.3) leads to a Laplace equation for the pressure in the layer,

$$\Delta P = 0. \tag{2.4}$$

To complete the formulation of the problem, we need to specify the boundary conditions. Defining the position of the crack front to be $x = f(y)$, with $f(y) = 0$ corresponding to a straight front, we may write the boundary conditions as

$$u(x, y, 0) = v(x, y, 0) = w(x, y, 0) = 0, \tag{2.5}$$

$$\sigma_{xz}(x, y, 1) = \sigma_{yz}(x, y, 1) = 0, \tag{2.6}$$

$$w(x, y, 1) = h(x, y), \tag{2.7}$$

$$\sigma_{zz}(x, y, 1) = \begin{cases} \alpha^3 \Delta^2 h(x, y), & x < f(y), \\ 0, & x > f(y). \end{cases} \tag{2.8}$$

The conditions (2.5) reflect the attachment of the adhesive layer to the substrate $z=0$. The rest of the conditions are a consequence of the continuity of displacement and traction at the adhesive interface between the layer and the flexible cover-slip. In particular, conditions (2.6) follow from the assumption of a shear-free interface between the flexible plate and the adhesive layer. From a physical point of view, we argue that the separation between the plate and the film of order of a 'van der Waals' distance (approx. 5 nm) allows the plate to 'slip' relative to the layer so that the shear stresses are minimal; in reality, there is some evidence of slip, but the exact boundary condition is still a matter of some debate (Ghatak *et al.* 2005). As we will see later, this choice may be responsible for the small discrepancy between the theoretical prediction for the critical wavelength and that observed experimentally. Equations (2.7) and (2.8) state that the layer is in contact with the flexible plate, i.e. the cover-slip only in

the domain $x<f(y)$. We note that $\alpha=(D/\mu H^3)^{1/3}$, the ratio of the two characteristic length-scales is the only control parameter in the problem.

Far from the crack, the deflection of the elastic plate $h(x,y)$ and the stress at the interface $\sigma_{zz}(x,y,1)$ must also satisfy the asymptotic relations

$$h(x,y)=0 \quad \text{as} \quad x\to-\infty, \tag{2.9}$$

$$\sigma_{zz}(x,y,1)=\frac{\eta(y)}{\sqrt{\pi(f(y)-x)}}+O\Big(\sqrt{f(y)-x}\Big) \quad \text{as} \quad x\to f(y)^{-}. \tag{2.10}$$

The condition (2.9) ensures the decay of the traction and displacements far from the crack front, while (2.10) enforces the inverse square-root singularity of the stress field at the crack front, with $\eta(y)$ being the local stress intensity factor. Finally, we note that the vertical displacement of the cover-slip $h_{\mathrm{g}}(x,y)$ in the region where it is free ($x>f(y)$) satisfies the equation

$$\Delta^2 h_{\mathrm{g}}(x,y)=0, \tag{2.11}$$

with the boundary conditions

$$h_{\mathrm{g}}(a,y)=1, \tag{2.12}$$

$$\Delta h_{\mathrm{g}}(x,y)|_{x=a}=0, \tag{2.13}$$

where a is the dimensionless position of the spacer that lifts the cover-slip (see figure 1*a*). At the crack front, $x=f(y)$, the following continuity conditions hold

$$h(x,y)|_{x=f(y)^-}=h_{\mathrm{g}}(x,y)|_{x=f(y)}, \tag{2.14}$$

$$\nabla h(x,y)|_{x=f(y)^-}=\nabla h_{\mathrm{g}}(x,y)|_{x=f(y)}, \tag{2.15}$$

$$\Delta h(x,y)|_{x=f(y)^-}=\Delta h_{\mathrm{g}}(x,y)|_{x=f(y)}, \tag{2.16}$$

which correspond to the physical requirements that the displacement of the cover-slip (elastic plate), its gradient and its curvature are all continuous at this location. However, the derivative of the curvature, which is proportional to the vertical shear force will be discontinuous at the crack front.

The use of a long wavelength plate theory for the cover-slip, embodied in (2.8) needs to be justified, especially since we treat the adhesive film as a bulk solid, including the effect of the singular stress distribution at the crack tip. Two facts help us: (i) both faces of the cover-slip are free of shear stresses and thus allow it to deform by bending, while the adhesive film, which is stuck to the substrate and confined in the normal direction by the cover-slip can only deform isochorically by shearing and (ii) the three-dimensional effects of the singular stress on the cover-slip in the vicinity of the crack tip are relevant only in a boundary layer whose size scales as the thickness of the cover-slip (Keer & Silva 1972). Experimental observations show that the critical value of the confinement parameter for the onset of the undulatory instability $\alpha\sim\alpha_{\mathrm{c}}\approx 18$ so that the critical adhesive layer thickness $H_{\mathrm{c}}\approx h(E_{\mathrm{p}}/\mu)^{1/3}/40$, where we have used the fact that the bending stiffness of the cover-slip $D=E_{\mathrm{p}}h^3/12(1-\nu^2)$, where E_{p} and ν are the Young modulus and Poisson ratio of the glass cover-slip of thickness h. Since $E_{\mathrm{p}}\approx 100$ GPa, $\mu\approx 1$ MPa, $\nu\approx 0.25$, this yields $H_{\mathrm{c}}\approx h$. Thus, over scales much larger than the thickness of the cover-slip, we may use a simple plate theory to characterize its deformations, while we must account for the complete elastic field in the adhesive film.

The piecewise boundary condition (2.8) suggests that we change the coordinate system from (x, y, z) to $(X \equiv x - f(y), y, z)$. With respect to this system, we may then write

$$\frac{\partial}{\partial x} A(x, y, z) = \frac{\partial}{\partial X} A(X, y, z), \tag{2.17}$$

$$\frac{\partial}{\partial y} A(x, y, z) = \left[\frac{\partial}{\partial y} - f'(y)\frac{\partial}{\partial X}\right] A(X, y, z), \tag{2.18}$$

$$\Delta A(x, y, z) = \left[(1 + f'^2(y))\frac{\partial^2}{\partial X^2} - f''(y)\frac{\partial}{\partial X} - 2f'(y)\frac{\partial^2}{\partial y\,\partial X} + \frac{\partial^2}{\partial y^2} + \frac{\partial^2}{\partial z^2}\right] A(X, y, z). \tag{2.19}$$

Furthermore, we assume that the perturbed crack has the form $f(y) = \epsilon \sin \omega y$, with $|\epsilon| \ll 1$. Then, anticipating a perturbation expansion in ϵ to account for the undulations of the crack, we introduce the following forms

$$A(X, y, z) = A_0(X, z) + \epsilon\left[A_1(X, z) + \frac{\partial}{\partial X} A_0(X, z)\right] \sin \omega y + O(\epsilon^2), \tag{2.20}$$

$$B(X, y, z) = \epsilon B_1(X, z) \cos \omega y + O(\epsilon^2). \tag{2.21}$$

Here $A \equiv u,\ w,\ h,\ h_g,\ P,\ \sigma_{xx},\ \sigma_{zz},\ \sigma_{xz},\ \sigma_{yy}$, while $B \equiv v,\ \sigma_{xy},\ \sigma_{yz}$. The advantage of the form of these perturbation expansions is that it makes the equations for the zeroth- and first-order problem in ϵ similar; in particular, by changing the subscripts from 1 to 0, and taking the limit $\omega = 0$ allows us to deduce the zeroth-order system from the first-order one and provides some notational and computational efficiency in our algebraic manipulations. Substituting the forms (2.20) and (2.21) into the equilibrium equations in the film (2.2)–(2.4) yields

$$\frac{\partial P_1}{\partial X} = \frac{\partial^2 u_1}{\partial X^2} - \omega^2 u_1 + \frac{\partial^2 u_1}{\partial z^2}, \tag{2.22}$$

$$\omega P_1 = \frac{\partial^2 v_1}{\partial X^2} - \omega^2 v_1 + \frac{\partial^2 v_1}{\partial z^2}, \tag{2.23}$$

$$\frac{\partial P_1}{\partial z} = \frac{\partial^2 w_1}{\partial X^2} - \omega^2 w_1 + \frac{\partial^2 w_1}{\partial z^2}, \tag{2.24}$$

$$\frac{\partial u_1}{\partial X} - \omega v_1 + \frac{\partial w_1}{\partial z} = 0, \tag{2.25}$$

$$\frac{\partial^2 P_1}{\partial X^2} - \omega^2 P_1 + \frac{\partial^2 P_1}{\partial z^2} = 0, \tag{2.26}$$

subject to the boundary conditions (2.5)–(2.8) which may be written as

$$u_1(X, 0) = v_1(X, 0) = w_1(X, 0) = 0, \tag{2.27}$$

$$\sigma_{1Xz}(X, 1) = \sigma_{1yz}(X, 1) = 0, \tag{2.28}$$

$$w_1(X, 1) = h_1(X), \tag{2.29}$$

$$\sigma_{1zz}(X, 1) = \begin{cases} \alpha^3\left[\dfrac{\partial^2}{\partial X^2} - \omega^2\right]^2 h_1(X), & X < 0, \\ 0, & X > 0. \end{cases} \tag{2.30}$$

The above linear problem for P_1, u_1, v_1, w_1 may be solved in terms of Fourier transforms. In terms of the definitions

$$\tilde{A}(k,z) = \int_{-\infty}^{+\infty} A(X,z)\mathrm{e}^{\mathrm{i}kX}\mathrm{d}X, \quad A(X,z) = \int_{-\infty}^{+\infty} \tilde{A}(k,z)\mathrm{e}^{-\mathrm{i}kX}\frac{\mathrm{d}k}{2\pi}, \tag{2.31}$$

we may write the solution in the Fourier domain as

$$\tilde{P}_1(k,z) = a(k)\cosh(Kz) + b(k)\sinh(Kz), \tag{2.32}$$

$$\tilde{u}_1(k,z) = -\frac{\mathrm{i}k}{2K}\left(b(k)z\cosh(Kz) + (c(k)+a(k)z)\sinh(Kz)\right), \tag{2.33}$$

$$\tilde{v}_1(k,z) = \frac{\omega}{2K}\left(b(k)z\cosh(Kz) + \left(\frac{Kb(k)-k^2c(k)}{\omega^2} + a(k)z\right)\sinh(Kz)\right), \tag{2.34}$$

$$\tilde{w}_1(k,z) = \frac{1}{2}\left(a(k)z\cosh(Kz) - \left(\frac{a(k)}{K} - b(k)z\right)\sinh(Kz)\right), \tag{2.35}$$

where

$$K = \sqrt{k^2+\omega^2}. \tag{2.36}$$

These forms satisfy the equilibrium equations (2.22)–(2.26) and the boundary conditions at $z=0$ given by (2.27). Applying the boundary conditions (2.28) and (2.29) at $z=1$ leads to a relationship between $\tilde{\sigma}_{1zz}(k,1)$ and $\tilde{w}_1(k,1) = \tilde{h}_1(k)$ given by

$$\tilde{h}_1(k) = F(K)\tilde{\sigma}_{1zz}(k,1), \tag{2.37}$$

where

$$F(K) = \frac{-2K + \sinh 2K}{2K(1+2K^2+\cosh 2K)}. \tag{2.38}$$

The piecewise boundary condition (2.30) on $\sigma_{1zz}(x,1)$ suggests the use of the Wiener–Hopf method of factorization and solution. For this purpose we write

$$\tilde{h}_1(k) = \int_{-\infty}^{+\infty} h_1(X)\mathrm{e}^{\mathrm{i}kX}\mathrm{d}X = \tilde{h}_1^-(k) + \tilde{h}_1^+(k), \tag{2.39}$$

where

$$\tilde{h}_1^-(k) = \int_{-\infty}^{0} h_1(X)\mathrm{e}^{\mathrm{i}kX}\mathrm{d}X, \quad \tilde{h}_1^+(k) = \int_{0}^{+\infty} h_1(X)\mathrm{e}^{\mathrm{i}kX}\mathrm{d}X, \tag{2.40}$$

and

$$\tilde{\sigma}_{1zz}(k,1) \equiv \tilde{\sigma}_{1zz}^-(k,1) = \int_{-\infty}^{0} \sigma_{1zz}(X,1)\mathrm{e}^{\mathrm{i}kX}\mathrm{d}X, \tag{2.41}$$

where the condition $\sigma_{1zz}(X>0,1)=0$ has been used. We pause here to note that if k is complex ($k \equiv k_\mathrm{R} + \mathrm{i}k_\mathrm{I}$), the integrals in (2.40), (2.41) and their derivatives with respect to k are bounded at infinity only when $(k_\mathrm{I}X) > 0$. Therefore, in the complex k-plane, $\tilde{h}_1^+(k)$ is analytic when $\mathrm{Im}k > 0$, while $\tilde{h}_1^-(k)$ and $\tilde{\sigma}_{1zz}^-(k,1)$ are analytic when $\mathrm{Im}k < 0$. Then, in the Fourier domain, the boundary condition (2.30) may be written as

$$\tilde{\sigma}_{1zz}^-(k,1) = \alpha^3 G_1(k) + \alpha^3 K^4 \tilde{h}_1^-(k), \tag{2.42}$$

with

$$G_1(k) = h_1'''(0^-) - \mathrm{i}kh_1''(0^-) - (k^2+2\omega^2)h_1'(0^-) + \mathrm{i}k(k^2+2\omega^2)h_1(0^-). \tag{2.43}$$

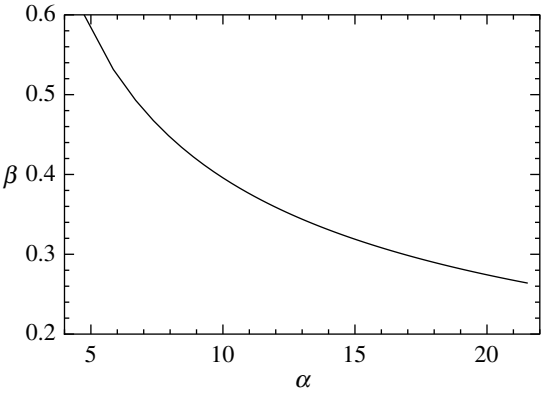

Figure 2. The solution $\beta(\alpha)$ of $C(K)=0$ as defined by (2.45).

Substituting the above expression for $\tilde{h}_1^-(k)$ in (2.37) leads to

$$\alpha^3 K^4 \tilde{h}_1^+(k) - \alpha^3 G_1(k) = C(K)\tilde{\sigma}_{1zz}^-(k,1), \tag{2.44}$$

where

$$C(K) = -1 + \alpha^3 K^4 F(K), \tag{2.45}$$

is a real function with the following properties: (i) it is an even function of K; (ii) as $K\to 0$, $C(K)\to -1+\alpha^3K^6/3$, and (iii) as $|K|\to\infty$, $C(K)\to\alpha^3|K|^3/2$. Therefore, $C(K)=0$ always admits two real roots $K=\pm\beta(\alpha)$ (see figure 2), which fact will be important for subsequent analysis. Thus, we may rewrite $C(K)$ as

$$C(K) = (K^2-\beta^2)D(K), \tag{2.46}$$

where $D(K)$ is an even function that has no real roots.

We now need to account for the asymptotic boundary conditions both far from and in the vicinity of the crack front. Since the front can undulate and thus is a free boundary, the similarity between the first-order problem and the zeroth-order problem stops here. For later reference, we note that the important equations for subsequent analysis are (2.43), (2.44) and (2.46), where the zeroth-order problems in ϵ are deduced by changing the subscripts from 1 to 0, and taking $\omega=0$.

The far-field condition (2.9) can be expressed in the Fourier domain as

$$\tilde{h}_0^{\pm}(k) = \text{cte} \quad \text{as} \quad k\to 0, \tag{2.47}$$

which is equivalent to the statement that $\tilde{h}_0^+(k)$ and $\tilde{h}_0^-(k)$ have no poles at $k=0$; the same condition holds for $\tilde{h}_1^{\pm}(k)$. The normal stress component at the interface between the plate and the adhesive film $\sigma_{zz}(X,y,1)$ may be written out as a perturbation expansion as

$$\sigma_{zz}(X,y,z) \equiv \sigma_{0zz}(X,z) + \epsilon\left[\sigma_{1zz}(X,z) + \frac{\partial}{\partial X}\sigma_{0zz}(X,z)\right]\sin(\omega y). \tag{2.48}$$

Additionally, the perturbation of the stress intensity factor $\eta(y)$ due to the shape perturbation of the crack may be written as

$$\eta(y) = \eta_0 + \epsilon\eta_1(\omega)\sin(\omega y) + O(\epsilon^2). \tag{2.49}$$

The stability of the straight crack front follows from the sign of the perturbed stress intensity factor (Rice 1985); if $\eta_1(\omega) > 0$, the straight front is stable, while if $\eta_1(\omega) < 0$ it is unstable.

In light of the crack-tip singularity as given by (2.10), the behaviour of $\sigma_{0zz}(X,1)$ and $\sigma_{1zz}(X,1)$ in the vicinity of the crack front $X=0$ are given by

$$\sigma_{0zz}(X,1) = \frac{\eta_0}{\sqrt{-\pi X}} + O(\sqrt{-X}) \quad \text{as} \quad X \to 0^-, \tag{2.50}$$

$$\sigma_{1zz}(X,1) + \frac{\partial}{\partial X}\sigma_{0zz}(X,1) = \frac{\eta_1(\omega)}{\sqrt{-\pi X}} + O(\sqrt{-X}) \quad \text{as} \quad X \to 0^-. \tag{2.51}$$

Equivalently in the Fourier domain, the behaviour of $\tilde{\sigma}^-_{0zz}(k,1)$ and $\tilde{\sigma}^-_{1zz}(k,1)$ for $|k| \to \infty$ are given by

$$\tilde{\sigma}^-_{0zz}(k,1) = \frac{\eta_0}{\sqrt{\mathrm{i}k}} + O\left(\frac{1}{(\mathrm{i}k)^{3/2}}\right) \quad \text{as} \quad |k| \to \infty, \tag{2.52}$$

$$\tilde{\sigma}^-_{1zz}(k,1) = \eta_0\sqrt{\mathrm{i}k} + O\left(\frac{1}{\sqrt{\mathrm{i}k}}\right) \quad \text{as} \quad |k| \to \infty, \tag{2.53}$$

so that the first-order perturbation of the stress intensity factor given by (2.51) is

$$\eta_1(\omega) = \lim_{|k|\to\infty} \sqrt{\mathrm{i}k}(\tilde{\sigma}^-_{1zz}(k,1) - \mathrm{i}k\tilde{\sigma}^-_{0zz}(k,1)). \tag{2.54}$$

Finally, the vertical displacement of the elastic plate $h_{\mathrm{g}}(X,y) = h_{\mathrm{g}}(X)$ in the region where it is free ($X>0$) can be determined by integrating (2.11) with the boundary conditions (2.12) and (2.13). In terms of the notation introduced at the beginning of this section, the zeroth-order solution $h_{\mathrm{g}0}(X)$ of the deflection of the plate is given by

$$h_{\mathrm{g}0}(X) = c_1(X-a)^3 + c_2(X-a) + 1, \tag{2.55}$$

where c_1 and c_2 are real constants. At the crack front, $X=0$, the continuity conditions (2.14)–(2.16) impose

$$h_0(0^-) = -c_1 a^3 - c_2 a + 1, \tag{2.56}$$

$$h_0'(0^-) = 3c_1 a^2 + c_2, \tag{2.57}$$

$$h_0''(0^-) = -6c_1 a. \tag{2.58}$$

For the first-order problem that accounts for the undulatory perturbations of the crack front, the deflection of the glass plate $h_{\mathrm{g}1}(X)$ is given by

$$h_{\mathrm{g}1}(X) = d_1(X-a)\cosh[\omega(X-a)] + d_2\sinh[\omega(X-a)], \tag{2.59}$$

where d_1 and d_2 are real constants. At the crack front, $X=0$, the continuity conditions (2.14)–(2.16) yield

$$h_1(0^-) = -d_1 a\cosh[\omega a] - d_2\sinh[\omega a], \tag{2.60}$$

$$h_1'(0^-) = (d_1 + d_2\omega)\cosh[\omega a] + d_1\omega a\sinh[\omega a], \tag{2.61}$$

$$h_1''(0^-) = \delta h_0'''(0) - d_1\omega^2 a\cosh[\omega a] - (2d_1 + d_2\omega)\omega\sinh[\omega a]. \tag{2.62}$$

We note that $\delta h_0'''(0) \equiv h_{\mathrm{g}0}'''(0) - h_0'''(0^-)$ due to the discontinuity of the derivative of the plate curvature at the crack front.

This completes the problem formulation. At each order of the perturbation, there are three constants of integrations and the stress intensity factor which

remain to be determined. For the zeroth-order problem, these quantities are c_1, c_2, $h_0'''(0^-)$ and η_0, while for the first-order problem they are d_1, d_2, $h_1'''(0^-)$ and η_1.

3. The straight front

We now turn to a solution of the straight front via the zeroth-order problem. Changing the subscripts from 1 to 0, and taking $\omega=0$ in (2.43) and (2.44) leads to

$$\alpha^3 k^4 \tilde{h}_0^+(k) - \alpha^3 G_0(k) = (k^2-\beta^2) D(k) \tilde{\sigma}_{0zz}^-(k,1), \tag{3.1}$$

$$G_0(k) = h_0^{-\prime\prime\prime}(0) - \mathrm{i}k h_0^{-\prime\prime}(0) - k^2 h_0^{-\prime}(0) + \mathrm{i}k^3 h_0^-(0). \tag{3.2}$$

Here $\tilde{\sigma}_{0zz}^-(k,1)$ is analytic for $\mathrm{Im}k<0$ and $\tilde{h}_0^+(k)$ is analytic for $\mathrm{Im}k>0$ suggesting the use of a Wiener–Hopf decomposition. Since the function $D(k)$ can be decomposed into the form (see appendix A)

$$D(k) = D_0^+(k) D_0^-(k), \tag{3.3}$$

where $D_0^+(k)$ (resp. $D_0^-(k)$) is analytic for $\mathrm{Im}k>0$ (resp. $\mathrm{Im}k<0$), (3.1) can be written as

$$\frac{\alpha^3 (k^4 \tilde{h}_0^+(k) - G_0(k))}{(k^2-\beta^2) D_0^+(k)} = D_0^-(k) \tilde{\sigma}_{0zz}^-(k,1), \tag{3.4}$$

which is an equality on the real axis between an analytic function for $\mathrm{Im}k>0$ (the left-hand side of (3.4)) and an analytic function for $\mathrm{Im}k<0$ (the right-hand side of (3.4)). The only analytic function in the complex plane that satisfies this property is a polynomial function of k (Muskhelishvili 1953). The asymptotic behaviour of $\tilde{\sigma}_{0zz}^-(k,1)$ given by (2.52), and the property that $D_0^-(k) \simeq \sqrt{\mathrm{i}k}$ for $|k|\to\infty$ (see appendix A) allows only a real constant as the general solution of (3.4), so that

$$\tilde{\sigma}_{0zz}^-(k,1) = \frac{\eta_0}{D_0^-(k)}, \tag{3.5}$$

$$\tilde{h}_0^+(k) = \frac{1}{k^4}\left[G_0(k) + \frac{\eta_0}{\alpha^3}(k^2-\beta^2) D_0^+(k) \right], \tag{3.6}$$

where η_0 is the stress intensity factor of the straight crack front.

Finally, substituting (3.6) into the Fourier-domain equivalents of (2.56)–(2.58), and noting that $\tilde{h}_0^+(k)$ has no poles at $k=0$ leads to the determination of the constants c_1, c_2, $h_0'''(0^-)$ and η_0 as functions of a and α with

$$c_1 = -\mathrm{i} D_0^{+\prime}(0) \frac{\beta^2 \eta_0}{6a\alpha^3}, \tag{3.7}$$

$$c_2 = (2D_0^+(0) + \beta^2 a \mathrm{i} D_0^{+\prime}(0) - \beta^2 D_0^{+\prime\prime}(0)) \frac{\eta_0}{2\alpha^3}, \tag{3.8}$$

$$\delta h_0'''(0) = h_{\mathrm{g}0}'''(0^+) - h_0'''(0^-) = -(aD_0^+(0) + \mathrm{i}D_0^{+\prime}(0)) \frac{\beta^2 \eta_0}{a\alpha^3}, \tag{3.9}$$

$$\eta_0 = \frac{6\alpha^3}{6aD_0^+(0) + (6+2\beta^2 a^2)\mathrm{i}D_0^{+\prime}(0) - 3\beta^2 a D_0^{+\prime\prime}(0) - \beta^2 \mathrm{i} D_0^{+\prime\prime\prime}(0)}. \tag{3.10}$$

In typical experiments where the degree of confinement is high, $a \gg 1$. Therefore, the stress intensity factor η_0 is well approximated by

$$\eta_0 \simeq \frac{3\alpha^3}{\beta^2 a^2 \mathrm{i} D_0^{+\prime}(0)}. \tag{3.11}$$

We are now in a position to find the equilibrium configuration of the straight front. The total dimensionless energy E_0 of the system is the sum of the energy in the adhesive film, that of the elastic plate and the interface, and is given by

$$\frac{2H^3}{D\delta^2}\,U_0 = E_0(a) = \frac{1}{\alpha^3}\int \mathrm{d}S\sigma_{0ij}\frac{\partial u_0 i}{\partial x_j} + \int \mathrm{d}x(h''_{\mathrm{g}0}(x))^2 + \Gamma a. \tag{3.12}$$

Here $\Gamma = 2\gamma H^4/D\delta^2$ is the dimensionless line tension (or equivalently the surface energy of the cohesive interface) with γ the dimensional surface energy. By using the divergence theorem and the far-field boundary conditions, the previous expression is simplified to

$$E_0(a) = -\frac{1}{\alpha^3}\int_{-\infty}^{0} \mathrm{d}x\sigma_{0zz}h_0(x) + \int_{-\infty}^{\infty} \mathrm{d}x(h''_{\mathrm{g}0}(x))^2 + \Gamma a. \tag{3.13}$$

Simplifying further, by integrating by parts and using the boundary conditions (2.8), (2.12) and (2.13) give

$$E_0(a) = -h_{\mathrm{g}0}(a)h'''_{\mathrm{g}0}(a) + h_{\mathrm{g}0}(0)\delta h'''_0(0) + \Gamma a. \tag{3.14}$$

For the asymptotic case $a \gg 1$, this yields

$$E_0(a) = \frac{3}{a^3} + \Gamma a. \tag{3.15}$$

The equilibrium position of the straight front with respect to the position of the spacer, a_{c}, is determined by minimizing $E_0(a)$ with respect to a and yields

$$a_{\mathrm{c}} = \left(\frac{9}{\Gamma}\right)^{1/4}. \tag{3.16}$$

We observe that the limiting case $a \gg 1$ corresponds to $\Gamma \ll 1$, a result going back to the work of Obreimoff (1930) who used the peeling of a thin film of mica to determine the value of the interfacial energy. In this limit, the dimensional crack length is given by $a_{\mathrm{c}}H = (9D\delta^2/2\gamma)^{1/4}$, which is independent of μ and H and thus of the properties of the adhesive elastic layer.

The above analysis also allows us to compute the crack opening stress $\sigma_{0zz}(x,1)$ given by

$$\sigma_{0zz}(x,1) = \eta_0 \int_{-\infty}^{+\infty} \frac{\mathrm{e}^{-\mathrm{i}kX}}{D_0^-(k)}\,\frac{\mathrm{d}k}{2\pi}, \tag{3.17}$$

which exhibits the usual square-root singularity at the crack tip. In figure 3, we plot $\sigma_{zz}(x,1)$ for different values of α. When $\alpha < \alpha_{\mathrm{b}} \simeq 9$, the stress decreases monotonically from the edge. However, when $\alpha > \alpha_{\mathrm{b}}$, we see that $\sigma_{zz}(x,1)$ becomes non-monotonic, with a new maximum at $x = x_{\mathrm{b}}$. An important point worth emphasizing here is the appearance of a threshold in the confinement parameter α_{b} that determines whether or not there is a secondary maximum in the stress behind the crack tip. Under certain conditions (Ghatak *et al.* 2004) corresponding to the case when the contact line is pinned by a perpendicular edge so that the singularity is weaker than that for a crack, crack nucleation proceeds via cavitation behind the pinned edge followed by the coalescence and growth of these resulting bubbles. A simple lubrication theory that neglects the stress

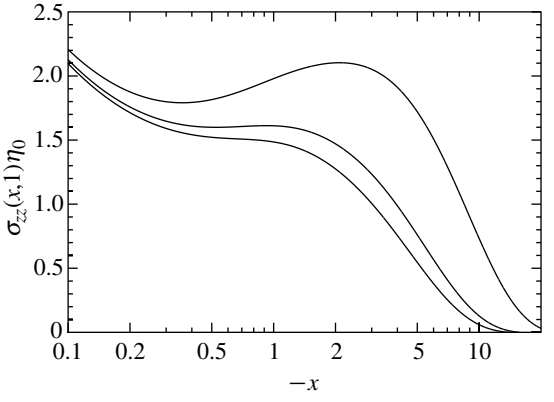

Figure 3. $\sigma_{zz}(x,1)/\eta_0$ for different values of α (from bottom to top $\alpha = 8, 10, 22$). We see that $\sigma_{zz}(x,1)/\eta_0$ displays a local maximum behind the crack tip when $\alpha > \alpha_b \simeq 9$.

singularity at the crack tip (Ghatak *et al.* 2004) suffices to capture this phenomena and yields predictions that are consistent with experiments. Since the local energy release rate at a perpendicular edge vanishes and furthermore, the incipient crack is pinned at the edge by inhomogeneities and defects it is prevented from moving. Then, cavitation bubbles may arise where the stress is maximally tensile behind the pinned crack tip. In the current situation, the crack tip (or contact line) is not pinned so that in general we do not expect cavitation behind the crack tip since the stresses at the tip will typically always be larger than that behind for two reasons: the contact line is a location where the energy release rate is finite (tantamount to the presence of a classical square-root singularity), and there are typically no pinning sites along the featureless adhesive surface, unlike at an edge.

In figure 4, we plot the dimensionless location of maximum tensile stress x_b as a function of the confinement parameter α. We see that x_b varies quasi-linearly with α for $\alpha \gtrsim 10$, with the dimensionless location of maximum tensile stress $-x_b \approx 0.1\alpha$. Then, the actual location of bubble nucleation is given by $-x_b H \approx 0.1(D/\mu)^{1/3}$ which is independent of the thickness of the film. For comparison, we also show the theoretically determined and experimentally observed dimensionless location of the maximum tensile stress for the case when the crack front is pinned at an edge (Ghatak *et al.* 2004). The main differences between these results can be traced back to the conditions at the crack front, embodied in (i) the effect of the crack-tip singularity and (ii) the implicit assumption in Ghatak *et al.* (2004) of a pinned crack tip that is not allowed to move.

4. The wavy front

We now consider the first-order problem that accounts for the undulatory perturbations of the crack front. To facilitate the application of the Wiener–Hopf method here, we write the function $G_1(k)$ given by (2.43) as

$$G_1(k) = (a_0 + \mathrm{i}a_1 k)(k - \mathrm{i}\omega)^2 + (b_0 + \mathrm{i}b_1 k)(k^2 + \omega^2 - \beta^2), \tag{4.1}$$

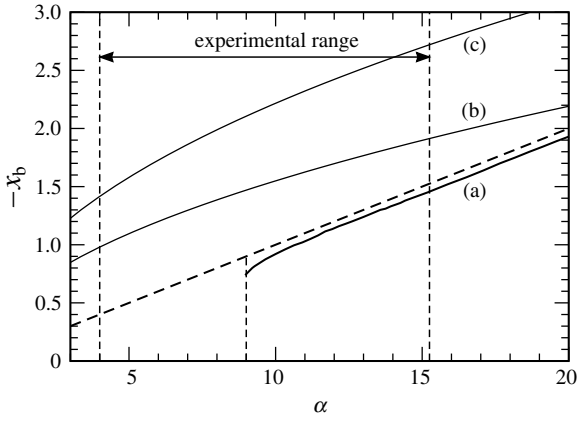

Figure 4. A comparison of the experiments and predictions for the location x_b of the secondary maximum in the normal stress $\sigma_{zz}(x,1)$ in the case treated here when the contact line (crack front) is free, and the case when it is pinned (Ghatak *et al.* 2004), as a function of the confinement parameter α. Curve (a) corresponds to the present work and the dashed line is given by $-x_b \approx 0.1\alpha$. Curve (b) corresponds to the theoretical results based on lubrication theory in Ghatak *et al.* (2004) and is given by $-x_b = 0.49\sqrt{\alpha}$. Curve (c) corresponds to the experimental results in Ghatak *et al.* (2004) and is given by $-x_b = 0.73\sqrt{\alpha} - 0.006\alpha$. We note that the present work shows that the secondary maximum appears only when $\alpha \geq \alpha_b$, and is a direct consequence of accounting for the crack-tip singularity.

where a_0, a_1, b_0 and b_1 are real constants related to $h_1(0^-)$, $h_1'(0^-)$, $h_1''(0^-)$ and $h_1'''(0^-)$ by

$$h_1(0^-) = a_1 + b_1, \tag{4.2}$$

$$h_1'(0^-) = -a_0 - 2\omega a_1 - b_0, \tag{4.3}$$

$$h_1''(0^-) = 2\omega a_0 + 3\omega^2 a_1 + (\omega^2 + \beta^2) b_1, \tag{4.4}$$

$$h_1'''(0^-) = -3\omega^2 a_0 - 4\omega^3 a_1 - (\omega^2 + \beta^2) b_0. \tag{4.5}$$

The boundary condition expressing traction continuity at the adhesive interface (2.44) may now be written as

$$\frac{(k+\mathrm{i}\omega)^2 \tilde{h}_1^+(k) - a_0 - \mathrm{i}a_1 k}{k^2 + \omega^2 - \beta^2} - \frac{D(K)\tilde{\sigma}_{1zz}^-(k,1)}{\alpha^3 (k - \mathrm{i}\omega)^2} = \frac{b_0 + \mathrm{i}b_1 k}{(k-\mathrm{i}\omega)^2}, \tag{4.6}$$

where the function $\tilde{\sigma}_{1zz}^-(k,1)$ is analytic for $\mathrm{Im}k < 0$ and the function $\tilde{h}_1^+(k)$ is analytic for $\mathrm{Im}k > 0$. Furthermore, since the function $D(K)$ can be decomposed into the form (see appendix A)

$$D(K) = D_1^+(k) D_1^-(k), \tag{4.7}$$

where $D_1^+(k)$ (resp. $D_1^-(k)$) is analytic for $\mathrm{Im}k > 0$ (resp. $\mathrm{Im}k < 0$), (4.6) can be written as

$$\frac{(k+\mathrm{i}\omega)^2 \tilde{h}_1^+(k) - a_0 - \mathrm{i}a_1 k}{(k^2 + \omega^2 - \beta^2) D_1^+(k)} - \frac{D_1^-(k)\tilde{\sigma}_{1zz}^-(k,1)}{\alpha^3 (k - \mathrm{i}\omega)^2} = \frac{b_0 + \mathrm{i}b_1 k}{(k-\mathrm{i}\omega)^2 D_1^+(k)}. \tag{4.8}$$

The left-hand side of (4.8) is the real-valued difference between a function that is analytic when $\mathrm{Im}k > 0$ and another function that is analytic when $\mathrm{Im}k < 0$. This

allows us to write the solutions for $\tilde{\sigma}^{-}_{1zz}(k,1)$ and $\tilde{h}^{+}_{1}(k)$ as (Muskhelishvili 1953)

$$\tilde{\sigma}^{-}_{1zz}(k,1) = \frac{\alpha^3(k-\mathrm{i}\omega)^2}{D^{-}_{1}(k)} \int_{-\infty}^{+\infty} \frac{\Phi(k',\omega)}{k'-k+\mathrm{i}\epsilon} \frac{\mathrm{d}k'}{2\mathrm{i}\pi}, \tag{4.9}$$

$$\tilde{h}^{+}_{1}(k) = \frac{a_0+\mathrm{i}a_1k}{(k+\mathrm{i}\omega)^2} + \frac{(k^2+\omega^2-\beta^2)D^{+}_{1}(k)}{(k+\mathrm{i}\omega)^2} \int_{-\infty}^{+\infty} \frac{\Phi(k',\omega)}{k'-k-\mathrm{i}\epsilon} \frac{\mathrm{d}k'}{2\mathrm{i}\pi}, \tag{4.10}$$

where

$$\Phi(k',\omega) = \frac{b_0+\mathrm{i}b_1k'}{(k'-\mathrm{i}\omega)^2 D^{+}_{1}(k')}. \tag{4.11}$$

The function $D^{+}_{1}(k')$ is analytic when $\mathrm{Im}k'>0$ so that $\Phi(k',\omega)$ is analytic when $\mathrm{Im}k'>0$ except at $k'=\mathrm{i}\omega$ where it exhibits a pole of multiplicity 2. This property allows us to evaluate the integrals in (4.9) and (4.10) leading to

$$\tilde{\sigma}^{-}_{1zz}(k,1) = -\frac{\alpha^3}{D^{-}_{1}(k)} \left[\frac{\partial}{\partial k'} \left[\frac{b_0+\mathrm{i}b_1k'}{D^{+}_{1}(k')} \right]_{k'=\mathrm{i}\omega} (k-\mathrm{i}\omega) + \frac{b_0-b_1\omega}{D^{+}_{1}(\mathrm{i}\omega)} \right]. \tag{4.12}$$

To complete the solution of the wavy front problem, we need to fix the real constants d_1, d_2 and $h^{-\prime\prime\prime}_{1}(0)$. The other constants introduced during the analysis are determined *a posteriori* through (2.60)–(2.62) and (4.2)–(4.5). First, we note that (2.42) yields

$$\tilde{h}^{-}_{1}(k) = \frac{\tilde{\sigma}^{-}_{1zz}(k,1)-\alpha^3 G_1(k)}{\alpha^3(k^2+\omega^2)^2}. \tag{4.13}$$

Since $\tilde{h}^{-}_{1}(k)$ is analytic for $\mathrm{Im}k<0$, there cannot be any poles at $k=-\mathrm{i}\omega$, leading to the conditions

$$\tilde{\sigma}^{-}_{1zz}(-\mathrm{i}\omega,1)-\alpha^3 G_1(-\mathrm{i}\omega) = 0, \tag{4.14}$$

$$\frac{\partial}{\partial k}[\tilde{\sigma}^{-}_{1zz}(k,1)-\alpha^3 G_1(k)]_{k=-\mathrm{i}\omega} = 0. \tag{4.15}$$

Using our knowledge of the singularity at the crack tip which implies that $\tilde{\sigma}^{-}_{1zz}(k,1) \sim \eta_0\sqrt{(\mathrm{i}k)}$ for $|k|\to\infty$ (see (2.53)) and the asymptotic behaviour of $D^{-}_{1}(k) \simeq \sqrt{\mathrm{i}k}$ for $|k|\to\infty$ (see appendix A) in (4.12) leads to

$$\mathrm{i}\frac{\partial}{\partial k'} \left[\frac{b_0+\mathrm{i}b_1k'}{D^{+}_{1}(k')} \right]_{k'=\mathrm{i}\omega} = \frac{\eta_0}{\alpha^3}. \tag{4.16}$$

The conditions (4.14)–(4.16) determine the constants d_1, d_2 and $h^{-\prime\prime\prime}_{1}(0)$ as functions of a, α, ω and η_0, but we will not write them out explicitly due to their length. Instead, to understand the onset of the wavy instability of the crack front, we will focus on the determination of the perturbation to the stress intensity factor $\eta_1(\omega)$ induced by the perturbation of the crack front given by (2.49) and (2.54). For this, we first simplify the expression for $\tilde{\sigma}^{-}_{1zz}(k,1)$, by using the condition (4.16) and write (4.12) as

$$\tilde{\sigma}^{-}_{1zz}(k,1) = \frac{\eta_0}{D^{-}_{1}(k)}(\mathrm{i}k+\omega+\kappa(\omega)), \tag{4.17}$$

where

$$\kappa(\omega) = \frac{\alpha^3(\omega b_1-b_0)}{\eta_0 D^{+}_{1}(\mathrm{i}\omega)}. \tag{4.18}$$

When $a \gg 1$, some algebra allows us to show that $\kappa(\omega)$ is simply given by

$$\kappa(\omega) = \frac{D_1^+(\mathrm{i}\omega) - D_0^+(0)}{\mathrm{i}D_1^{+\prime}(\mathrm{i}\omega) + \frac{2\omega}{\beta^2} D_1^+(\mathrm{i}\omega)}, \tag{4.19}$$

where the parameter $\beta(\alpha)$ is plotted in figure 2. Finally, (2.54), (3.5) and (4.17) allow us to determine the perturbation to the stress intensity factor

$$\eta_1(\omega) = (\omega + \kappa(\omega) + \theta(0) - \theta(\omega))\eta_0, \tag{4.20}$$

where $\theta(\omega)$ is defined by the asymptotic expansion

$$D_1^-(k) = \sqrt{\mathrm{i}k}\left(1 + \frac{\theta(\omega)}{\mathrm{i}k}\right) \quad \text{as} \quad |k| \to \infty. \tag{4.21}$$

To understand the criterion for instability in terms of the perturbed stress intensity factor (Rice 1985), we note that if $\eta_1 > 0$, regions which are further away from the spacer ($\sin(\omega y) < 0$) have a stress intensity factor $\eta(y)$ which is smaller than regions which are closer ($\sin(\omega y) > 0$). Thus, as the crack advances quasi-statically the undulations will diminish and the crack front will tend to straighten and stabilize. On the other hand, if $\eta_1 < 0$ regions which are further away from the spacer ($\sin(\omega y) < 0$) have a stress intensity factor $\eta(y)$ that is larger than regions which are closer ($\sin(\omega y) > 0$) leading to a destabilizing effect. Evaluating $\eta_1(\omega)$ asymptotically using the expression (4.20) and the asymptotic expansions of $\kappa(\omega)$ and $\theta(\omega)$ yields

$$\eta_1(\omega)/\eta_0 \simeq 2\omega, \quad \omega \ll 1,$$

$$\eta_1(\omega)/\eta_0 \simeq \omega/2, \quad \omega \gg 1.$$

Therefore, the straight front is always stable to both small and large wavelength perturbations for all values of the confinement parameter α. When $\omega \ll 1$, corresponding to long wavelength perturbations (relative to the film thickness), there is no energetic gain in having a curved crack, while for very short wavelength perturbations ($\omega \gg 1$), confinement plays no role, and in the absence of any intrinsic short length-scale these perturbations are also stable. Thus, when α is small, $\eta_1(\omega)$ increases monotonically. However, as α increases, this relation becomes non-monotonic owing to the effects of boundary-induced elastic shielding. Eventually, when $\alpha = \alpha_c$ the perturbation in the stress intensity factor η_1 changes sign for finite non-zero ω, yielding an unstable wavelength $\lambda = 2\pi/\omega$.

To quantify this, we compute $\eta_1(\omega)$ as given by (4.20) using the definitions (4.19) and (4.21) of $\kappa(\omega)$ and $\theta(\omega)$. These quantities are computed numerically in terms of the decomposition of $D(K)$ into $D_1^+(k)D_1^-(k)$ (see appendix A), yielding the results shown in figure 5, where we plot $\eta_1(\omega)$ for different values of α. We see that there is a critical value $\alpha = \alpha_c \simeq 21$ for which $\eta_1(\omega_c) = 0$ with the wavenumber of the instability $\omega_c \simeq 1.85$, which corresponds to a wavelength $\lambda_c \simeq 3.4H$ in reasonable agreement with the corresponding experimental values of $\alpha_{\mathrm{exp}} \simeq 18$, $\omega_{\mathrm{exp}} \simeq 1.57$ and $\lambda_{\mathrm{exp}} \sim 4H$ (Ghatak & Chaudhury 2003). The small discrepancy (of order 15%) for both the wavelength and the threshold is probably due to the uncertainty in our knowledge of detailed nature of the adhesive contact. In particular, it is not clear that the condition of zero tangential slip (2.6) between the glass plate and the adhesive film is accurate, owing to the relatively weak nature of the van der Waals interactions present (Ghatak *et al.* 2004).

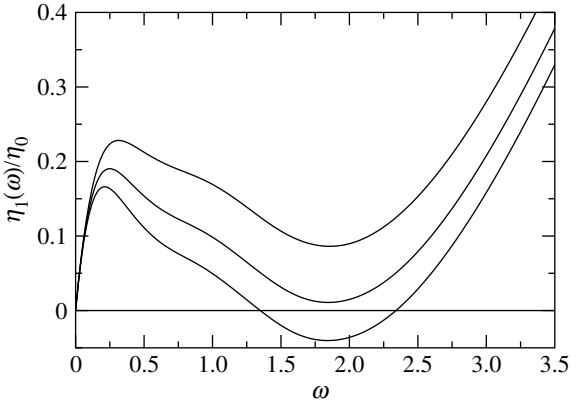

Figure 5. $\eta_1(\omega)/\eta_0$ for different values of α (from top to bottom $\alpha = 15, 20, 25$). We see that η_1/η_0 becomes negative for $\alpha > \alpha_w \simeq 21$ and indicates the threshold for the onset of the undulatory instability of the crack front. The corresponding value of the dimensionless wavenumber $\omega_c \approx 1.85$.

5. Discussion

Our study illuminates the crucial role of geometric confinement in quasi-static fracture problems. In particular, we show how a straight crack front may lose stability in the plane of the interface due to a competition between bulk and surface effects in the presence of multiple length-scales. This must be contrasted with the instability of the crack plane itself to transverse out-of-plane undulations in such examples as the sinusoidal cracking of a thin glass plate (Yuse & Sano 1993; Adda-Bedia & Pomeau 1995).

In the context of adhesion of flexible plates to soft confined films, our analysis allowed us to determine the equilibrium configuration of the straight front, as well as the conditions for and the mechanism of the instability of a straight crack to in-plane perturbations. In particular, we find that the equilibrium position of the straight front does not depend on either the material properties or the thickness of the adhesive film. Our analysis in this case generalizes the classical analysis of Obreimoff (1930) for peeling a solid (mica) film from the bulk material via cleavage by considering the case when the confinement parameter α is not large. As the degree of confinement is increased, the normal traction at the adhesive interface displays a secondary maximum behind the crack front when $\alpha > \alpha_b \simeq 9$. The location of this secondary stress maximum x_b is essentially independent of the thickness of the film, with $-x_b H = 0.1(D/\mu)^{1/3}$. However, since $-x_b H \ll \alpha$, in the present case where the crack front is free to move to its equilibrium position unhindered, the singularity at the crack tip dominates the stress field and bubble nucleation does not occur. When confinement is increased still further, we see the onset of an undulatory instability of the crack occurring when $\alpha > \alpha_c = 21$, in agreement with experiments (Ghatak *et al.* 2000; Ghatak & Chaudhury 2003). We find that the wavelength of the instability scales linearly with the thickness H, consistent with experiments, although there is a quantitative discrepancy with the actual prefactor that shows a difference of about 15%, which may be due to the

experimental difficulty of controlling the tangential slippage of the flexible plate on the adhesive film.

On the other hand, when the crack tip is pinned at an edge of adhesive film (e.g. Ghatak *et al.* 2004), the elastic layer spans the region $X<0$ only, and the two effects conspire to change the qualitative nature of the stress field: the crack tip is blunted and pinned strongly to the edge. This is consistent with other experiments reported in Ghatak *et al.* (2004) where the effect of a change in the angle of the edge that pins a crack was to change the relative importance of pinning and the crack-tip stress singularity, leading to a suppression of the tendency for bubble nucleation. This is also why the simple elastic lubrication theory in Ghatak *et al.* (2004) that ignores the stress singularity at the crack tip completely, but implicitly assumes that the crack is pinned at the edge of the adhesive film yields criteria for bubble nucleation that compare well with experiments (see figure 4), but cannot provide a critical value of the confinement parameter α_{b} for bubble nucleation.

Taken together, these results show that by controlling confinement and crack pinning, it is possible to quantitatively understand and thus tailor the toughness of interfaces using simple geometric attributes. Much still remains to be accomplished in theoretical, experimental and technological arenas.

We thank John Hinch for his many comments that helped to sharpen and clarify our arguments. This work was supported by the Schlumberger Chair Fund at University of Cambridge (L.M.). Laboratoire de Physique Statistique de l'Ecole Normale Supérieure is associated with the CNRS (UMR 8550) and Universities Paris VI and Paris VII.

Appendix A. The Wiener–Hopf decomposition of $D(K)$

Here we present the method of decomposition of the function $D(K)$ defined in (2.46) for the zeroth- and first-order problem. Using the properties of the function $C(K)$ defined in (2.45), we define a new function $E(K)$ such that

$$E(K) = \frac{2D(K)}{\alpha^3\sqrt{\gamma^2+K^2}} = \frac{2C(K)}{\alpha^3(K^2-\beta^2)\sqrt{\gamma^2+K^2}}, \tag{A 1}$$

where

$$\gamma = \frac{2}{\alpha^3\beta^2}.$$

The function $E(K)$ is an even real function of K that satisfies $E(0)=1$ with $E(K)\to 1$ as $|K|\to\infty$. These properties allow to approximate $E(K)$ using a numerical scheme introduced by Liu & Marder (1991). We first define a new variable l such that

$$K = \frac{bl}{\sqrt{1-l^2}}. \tag{A 2}$$

Now the function $E(l)$ is a bounded non-oscillatory function on $[-1,1]$. The constant b is chosen such that $E(l)$ is well behaved. The function $E(l)$ is approximated to any desired accuracy as a sum of Chebyshev polynomials. The complex roots l_n of $E(l)$ are then found numerically. Using these results and the

properties of the function $E(l)$, we write $E(l)$ in the following approximate form

$$E(l) \simeq \prod_{n=1}^{N}(l^2 - l_n^2) \Rightarrow E(K) \simeq \prod_{n=1}^{N} \frac{K^2 + \beta_n^2}{K^2 + b^2}, \tag{A 3}$$

where

$$\beta_n = \frac{bl_n}{\sqrt{l_n^2 - 1}}. \tag{A 4}$$

We now use the property $D(k) = D(-k)$ so that it follows that

$$\Rightarrow D_0^+(k)D_0^-(k) = D_0^+(-k)D_0^-(-k) \Rightarrow \frac{D_0^+(k)}{D_0^-(-k)} = \frac{D_0^+(-k)}{D_0^-(k)} = \text{const.},$$

where the constant is arbitrary. The same property holds for the first-order decomposition. Therefore, the Wiener–Hopf decomposition of the zeroth- and first-order problem can now be carried out without any difficulty. For the zeroth order, one has

$$D_0^-(k) = \sqrt{\gamma + \mathrm{i}k}E_0^-(k), \tag{A 5}$$

$$D_0^+(k) = \frac{\alpha^3}{2}\sqrt{\gamma - \mathrm{i}k}E_0^+(k), \tag{A 6}$$

where we have chosen the constant such that $D_0^-(k) \sim \sqrt{\mathrm{i}k}$ for $|k| \to \infty$, and

$$E_0^{\mp}(k) = \prod_{n=1}^{N} \frac{\beta_n \pm \mathrm{i}k}{b \pm \mathrm{i}k}. \tag{A 7}$$

For the first order, one has

$$D_1^-(k) = \sqrt{\sqrt{\gamma^2 + \omega^2} + \mathrm{i}k}E_1^-(k), \tag{A 8}$$

$$D_1^+(k) = \frac{\alpha^3}{2}\sqrt{\sqrt{\gamma^2 + \omega^2} - \mathrm{i}k}E_1^+(k), \tag{A 9}$$

where

$$E_1^{\mp}(k) = \prod_{n=1}^{N} \frac{\sqrt{\beta_n^2 + \omega^2} \pm \mathrm{i}k}{\sqrt{b^2 + \omega^2} \pm \mathrm{i}k}. \tag{A 10}$$

Finally, the quantities needed for computing the first-order calculations are given by

$$\theta(\omega) = \frac{1}{2}\sqrt{\gamma^2 + \omega^2} + \sum_{n=1}^{N}\left[\sqrt{\beta_n^2 + \omega^2} - \sqrt{b^2 + \omega^2}\right], \tag{A 11}$$

$$D_1^+(\mathrm{i}\omega) = \frac{\alpha^3}{2}\sqrt{\sqrt{\gamma^2 + \omega^2} + \omega}\prod_{n=1}^{N} \frac{\sqrt{\beta_n^2 + \omega^2} + \omega}{\sqrt{b^2 + \omega^2} + \omega}, \tag{A 12}$$

$$\frac{\mathrm{i}D_1^{+\prime}(\mathrm{i}\omega)}{D_1^+(\mathrm{i}\omega)} = \frac{1}{2(\sqrt{\gamma^2 + \omega^2} + \omega)} + \sum_{n=1}^{N}\left[\frac{1}{\sqrt{\beta_n^2 + \omega^2} + \omega} - \frac{1}{\sqrt{b^2 + \omega^2} + \omega}\right]. \tag{A 13}$$

References

Adda-Bedia, M. & Pomeau, Y. 1995 Crack instabilities of a heated glass strip. *Phys. Rev. E* **52**, 4105–4113. (doi:10.1103/PhysRevE.52.4105)

Conley, K. M., Gu, W., Ritter, J. E. & Lardner, T. J. 1992 Observations on finger-like crack growth at a urethane acrylate/glass interface. *J. Adhes.* **39**, 173–184.

Fields, R. J. & Ashby, M. F. 1976 Finger-like crack growth in solids and liquids. *Phil. Mag.* **33**, 33–38.

Ghatak, A. 2005 Confinement induced instability of thin elastic film. http://arxiv.org/abs/cond-mat/0505045.

Ghatak, A. & Chaudhury, M. K. 2003 Adhesion induced instability patterns in thin confined elastic film. *Langmuir* **19**, 2621–2631. (doi:10.1021/la026932t)

Ghatak, A., Shenoy, V., Chaudhury, M. K. & Sharma, A. 2000 Meniscus instability in thin elastic film. *Phys. Rev. Lett.* **85**, 4329–4332. (doi:10.1103/PhysRevLett.85.4329)

Ghatak, A., Mahadevan, L., Chung, J. Y., Chaudhury, M. K. & Shenoy, V. 2004 Peeling from a biomimetically patterned thin elastic film. *Proc. R. Soc. A* **460**, 2725–2735. (doi:10.1098/rspa.2004.1313)

Ghatak, A., Mahadevan, L. & Chaudhury, M. K. 2005 Measuring the work of adhesion between a soft confined film and a flexible plate. *Langmuir* **21**, 1277–1281. (doi:10.1021/la0484826)

Keer, L. & Silva, M. A. G. 1972 Two mixed problems of a semi-infinite layer. *J. Appl. Mech.* **39**, 1121–1124.

Liu, X. & Marder, M. 1991 The energy of a steady-state crack in a strip. *J. Mech. Phys. Solids* **39**, 947–961. (doi:10.1016/0022-5096(91)90013-E)

McEwan, A. D. & Taylor, G. I. 1966 The peeling of a flexible strip attached by a viscous adhesive. *J. Fluid Mech.* **26**, 1–15. (doi:10.1017/S0022112066001058)

Monch, W. & Herminghaus, S. 2001 Elastic instability of rubber films between solid bodies. *Europhys. Lett.* **53**, 525–531. (doi:10.1209/epl/i2001-00184-7)

Muskhelishvili, N. I. 1953 *Singular integral equations*. Groningen: Noordhoff.

Obreimoff, J. W. 1930 The splitting strength of mica. *Proc. R. Soc. A* **127**, 290–297.

Rice, J. R. 1985 First-order variation in elastic fields due to variation in location of a planar crack front. *J. Appl. Mech.* **107**, 571–579.

Saffman, P. G. & Taylor, G. I. 1958 The penetration of a fluid into a porous medium or Hele–Shaw cell containing a more viscous liquid. *Proc. R. Soc. A* **245**, 312–329.

Shenoy, V. & Sharma, A. 2002 Stability of a thin elastic film interacting with a contactor. *J. Mech. Phys. Solids* **50**, 1155–1173. (doi:10.1016/S0022-5096(01)00109-0)

Yuse, A. & Sano, M. 1993 Transition between crack patterns in quenched glass plates. *Nature* **362**, 329–331. (doi:10.1038/362329a0)